An Endogenously activated antiviral state restricts SARS-CoV-2 infection in differentiated primary airway epithelial cells

Lindsay Broadbent[1*], Connor G.G. Bamford[1], Guillermo Lopez Campos[1], Sheerien Manzoor[1], David Courtney[1], Ahlam Ali[1,2], Olivier Touzelet[1], Conall McCaughey[3], Ken Mills[2], Ultan F. Power[1*]

1. Wellcome-Wolfson Institute for Experimental Medicine, Queens University Belfast, Belfast, Northern Ireland, United Kingdom.

2. Patrick G Johnston Centre for Cancer Research, Queen's University Belfast, Belfast, UK.

3. Regional Virus Laboratory, Belfast Health and Social Care Trust, Belfast, Northern Ireland.

*Co-corresponding author

Abstract

Severe acute respiratory syndrome coronavirus 2 (SARS-CoV-2), the cause of the coronavirus disease-19 (COVID-19) pandemic, was identified in late 2019 and went on to cause over 3.3 million deaths in 15 months. To date, targeted antiviral interventions against COVID-19 are limited. The spectrum of SARS-CoV-2 infection ranges from asymptomatic to fatal disease. However, the reasons for varying outcomes to SARS-CoV-2 infection are yet to be elucidated. Here we show that an endogenously activated interferon lambda (IFNλ) pathway leads to resistance against SARS-CoV-2 infection. Using a well-differentiated primary nasal epithelial cell (WD-PNEC) model from multiple adult donors, we discovered that susceptibility to SARS-CoV-2 infection, but not respiratory syncytial virus (RSV) infection, varied. One of four donors was resistant to SARS-CoV-2 infection. High baseline IFNλ expression levels and associated interferon stimulated genes correlated with resistance to SARS-CoV-2 infection. Inhibition of the JAK/STAT pathway in WD-PNECs with high endogenous IFNλ secretion resulted in higher SARS-CoV-2 titres. Conversely, prophylactic IFNλ treatment of WD-PNECs susceptible to infection resulted in reduced viral titres. An endogenously activated IFNλ response, possibly due to genetic differences, may be one explanation for the differences in susceptibility to SARS-CoV-2 infection in humans. Importantly, our work supports the continued exploration of IFNλ as a potential pharmaceutical against SARS-CoV-2 infection.

Introduction

In late 2019 a novel coronavirus, severe acute respiratory syndrome coronavirus 2 (SARS-CoV-2), emerged in Hubei province in China [1,2]. This virus is the causative agent of the coronavirus disease-19 (COVID-19) pandemic, which has resulted in over 4.2 million deaths worldwide (as of August 2021). SARS-CoV-2 can infect people of any age. However, severe disease disproportionately affects older individuals or those with underlying health conditions. Clinical manifestations of SARS-CoV-2 infection range from asymptomatic or very mild symptoms to severe illness requiring hospitalization and death. COVID-19 disease is primarily a lung disease, typically manifesting itself as acute respiratory distress syndrome in severe cases, although extra-pulmonary complications, including cardiac, vascular, kidney and neurological pathologies, are also evident [3]. Furthermore, coagulopathies are commonly reported in COVID-19 disease patients. Reasons for the extreme variation in disease outcomes remain to be elucidated.

The upper respiratory tract is the primary site of SARS-CoV-2 infection. Infection can progress to the lower airways resulting in airway inflammation and potentially fatal pneumonia[1]. The major receptor for the viral spike protein (S), human angiotensin-converting enzyme 2 (ACE2), is expressed on airway epithelial cells but is also found on other tissue, including endothelial cells and smooth muscle cells[4]. Entry of the virus requires activation of the S glycoprotein by host proteases, such as furin and transmembrane serine protease 2 (TMPRSS2)[5]. SARS-CoV-2 is cytopathic to airway epithelial cells and alveolar cells. However, immune responses induced following infection are also thought to drive pathogenesis and disease severity in COVID-19. Chemokines and cytokines are released from infected tissues promoting leukocyte recruitment to the lungs, resulting in substantial inflammation in severe cases. Hallmarks of severe COVID-19 disease include high serum levels of IL-6, TNF-α, IP-10/CXCL10 and MCP-1, among others[6,7].

Dependent on viral, host and environmental factors, the IFN response to infection, and subsequent inflammation, can be either beneficial or deleterious to the individual. Type I and λ (type III) interferons (IFNs) are produced in response to viral infection. IFN-

mediated activation of the JAK-STAT pathway is responsible for the dramatic alteration in the cellular transcriptome and the activation of interferon-stimulated genes (ISGs), many of which have antiviral activities[8]. Patients with COVID-19 have low serum levels of type I and III IFNs but high levels of pro-inflammatory chemokines and cytokines[9]. However, it has been observed that higher serum IFN correlates positively with viral load and disease severity[10]. It is hypothesized that dysregulated, reduced or delayed IFN responses, in combination with high cytokine levels, results in more severe COVID-19 disease[11].

Unlike type I IFN receptors, the IFNλ receptor, IFNLR1, is not ubiquitously expressed and is present predominantly on epithelial cells at barrier tissues like the lungs and gastrointestinal tract[12]. As such, type III IFNs are considered to produce a more localised response to infection in comparison to the systemic inflammatory response often induced by type I IFN[13]. SARS-CoV-2 has been shown to induce an IFN response in epithelial cells, the timing of which is delayed with regard to peak viral replication. Pre-treatment of cells with IFNs is effective at blocking SARS-CoV-2 infection, and several directly anti-SARS-CoV-2 ISGs have been discovered, such as Ly6, OAS1 and IFITMs[14–16].

As the primary target of SARS-CoV-2 infection is the airway epithelium, models that authentically recreate the physiology and morphology of human airway epithelium *in vivo* will undoubtedly be important tools to address fundamental questions about human/SARS-CoV-2 interactions and subsequent innate immune responses. Therefore, in this study we report differential susceptibility to SARS-CoV-2 infection in well-differentiated primary nasal epithelial cell (WD-PNEC) cultures derived from adult donors. We obtained nasal brushings from 4 healthy donors with no previous history of SARS-CoV-2 infection. Interestingly, we found dramatically different susceptibility to SARS-CoV-2 infection, with 1 of the 4 donors being resistant. The resistance was likely mediated by high endogenous IFNL expression and associated ISG responses. These data may provide an explanation as to why some individuals experience asymptomatic infection following exposure to SARS-CoV-2.

Results

Resistance to SARS-CoV-2 infection in WD-PNECs

WD-PNEC cultures derived from 4 healthy adult donors demonstrated different susceptibility to SARS-CoV-2 infection and viral growth kinetics (Figure 1A). Following inoculation apical washes were harvested every 24 h post infection and titrated by plaque assay on Vero cells. WD-PNECs from 3 donors demonstrated similar SARS-CoV-2 growth kinetics with peak viral titres of $>10^6$ PFU/mL at 48 hpi followed by a plateau or decrease at 72 hpi. Surprisingly, infection of donor 122 did not result in productive infection of SARS-CoV-2, with virus titres continually diminishing relative to titres following inoculation. Immunofluorescence reinforced these results, with high levels of SARS-CoV-2 N expression in WD-PNECs from donors 311, 43 and 32, but with very few infected cells evident in those from donor 122 (Figure 1C). Consistent with other data, SARS-CoV-2 infection was restricted to the apical surface of the cultures[17]. To determine if resistance to infection was specific to SARS-CoV-2, we infected cultures derived from the same donors with respiratory syncytial virus (RSV), a RNA virus that primarily infects ciliated airway epithelium[18]. There was no evidence of restrictions in RSV growth kinetics in any donor. (Figure 1B).

Pre-activation of IFN pathway in resistant WD-PNECs

The timing and magnitude of IFN responses to SARS-CoV-2 infection is thought to play a role in disease severity. Transcriptomic analysis of RNA extracted at 48 and 96 hpi revealed that there was upregulation of genes associated with the IFNλ pathway in the mock-infected cultures of donor 122. Following SARS-CoV-2 infection the gene transcription signature of donor 122 did not significantly change (Figure 2A). Similar, or greater, levels of expression of *ACE2* and *TMPRSS2* were observed in this donor, confirming that resistance to infection was not due to absence or low expression of the attachment and entry factors needed for SARS-CoV-2 infection. This was confirmed by immunofluorescence (data not shown). The three donors susceptible to infection had similar patterns of gene expression, including an increase in expression of IFNλ-

associated genes following SARS-CoV-2 infection (Figure 2A). To confirm these results, IFNλ1 concentrations in basolateral medium from SARS-CoV-2- or mock-infected WD-PNECs (n=4 donors) were determined at 48 and 96 hpi. Increased IFNλ1 secretion was evident following infection at 96 hpi in cultures from donors 43 and 32, but not 311. In contrast, donor 122 cultures, which were not permissive to SARS-CoV-2 infection, had high levels of IFNλ1 (> 500 pg/mL) in the basolateral medium from mock-infected cultures at 48 and 96 hpi (Figure 2B). Transcriptomic analysis of the IFIH1-mediated interferon induction and toll-like receptor (TLR) signaling pathways revealed that donor 122 had a unique gene transcription signature compared to mock or infected cultures from the other donors (Supplementary Figure 1).

Pre-activation of IFN pathway and SARS-CoV-2 resistance phenotype are not transient.

To determine if the high baseline level of IFNλ1 in donor 122 cultures was an artifact of culture or the time at which the nasal brush was obtained, a second brush was taken 4 months after the first and cultured in the same manner. When fully differentiated the second cultures were infected with SARS-CoV-2, with similar results (Figure 3A). WD-PNECs cultured from the second nasal brush of donor 122 also had high endogenous levels of IFNλ (~400 pg/mL), albeit reduced compared to those evident in the cultures from the first brush. In contrast, IFNλ levels from mock-infected cultures from 6 other donors demonstrated background levels of secretion (Figure 3B).

IFN signaling restricts SARS-CoV-2 infection

SARS-CoV-2 is sensitive to exogenous IFN treatment [19]. We hypothesised that the high baseline level of IFNλ in basolateral medium of donor 122-derived WD-PNECs limited the spread of SARS-CoV-2 within the culture and prevented productive infection. Therefore, we blocked the major signalling pathway of IFNλ with the JAK1/2 inhibitor ruxolitinib prior to infection. WD-PNECs derived from a donor with low IFNλ secretion in response to SARS-CoV-2 infection (donor 311) was used as a control. Ruxolitinib treatment resulted in a massive increase in SARS-CoV-2 titres in apical washes from cultures derived from donor 122 (>3 $\log_{10}$ PFU/mL), reaching a peak titre of 7.6 $\log_{10}$ PFU/mL at 72 hpi (Fig.

159 4A). As expected, there was no significant effect of ruxolitinib treatment on donor 311,
160 which also reached peak viral titres at 72 hpi. Viral titres at 72 hpi were comparable for
161 untreated donor 311 cultures and ruxilitinib-treated donor 122 cultures, 7.78 and 7.6 $\log_{10}$
162 PFU/mL, respectively.

163 To demonstrate that IFNλ was the underlying cause of resistance to SARS-CoV-2
164 infection we replicated these conditions in the SARS-CoV-2 permissive donor 43. WD-
165 PNECs were pre-treated with IFNλ in the basolateral medium for 24 h prior to infection
166 (Figure 4B). Treatment with both 1 and 100 ng/mL IFNλ greatly reduced viral titres at 48
167 hpi by >2 $\log_{10}$ PFU/mL, resulting in titres similar to the input inoculum (4.18 $\log_{10}$
168 PFU/mL).

169 **Single nucleotide polymorphisms (SNP) analysis revealed differences in**
170 **pathogen sensing and interferon induction pathways unique to the resistant**
171 **donor**

172 Unbiased SNP analysis from our RNAseq data demonstrated clear differences between
173 donors, with unique variants in several genes in the SARS-CoV-2-resistant donor
174 compared to the permissive donors. Focusing our SNP analysis to selected genes
175 associated with antiviral responses, we identified 388 SNPs unique to donor 122 and a
176 further 33 present in donors 311, 43 and 32 but not detected in donor 122 (Figure 5A).
177 Further conditional filtering for quality and existing SNP (according to dbSNP, NIH)
178 identified 10 SNPs potentially involved in the high endogenous IFN secretion and
179 resistance to SARs-CoV-2 demonstrated by WD-PNECs derived from donor 122
180 (Figure 5B). Interestingly, SNPs unique to donor 122 were found in ADAR (rs3738032),
181 MAVS (rs2089960995), TLR1 (rs4833095), TLR2 (rs1816702; rs3804099) and TLR3
182 (rs3775296; rs3775291). SNPs present in all donors except 122 were found in ADAR
183 (rs1127313; rs1127326) and IFIH1 (rs1990760). Together these results show that
184 resistant versus permissive donors have unique constellations of SNPs that may cause
185 the molecular mechanisms of susceptibility or resistance to SARS-CoV-2 infection.

186

Discussion

The WD-PNEC model presents an ideal opportunity to study SARS-CoV-2 infection in a clinically relevant system. The upper respiratory epithelium is thought to be the initial site of infection for SARS-CoV-2[20]. As such, a comprehensive understanding of SARS-CoV-2 infection of nasal epithelium is critical to understanding the early events of the infection process, as they are likely influential in subsequent pathogenesis. Why some patients with COVID-19 experience no or mild symptoms consistent with an upper respiratory tract infection, while others experience much more severe symptoms often resulting in acute respiratory distress syndrome (ARDS) remains to be determined. Consistent with earlier reports, we demonstrated that differentiated nasal epithelial cells can be productively infected with SARS-CoV-2 and that infection is primarily restricted to the apical surface. Surprisingly, however, we provide robust evidence of differential susceptibility of airway epithelium to SARS-CoV-2 infection, with airway epithelium from some individuals being highly susceptible and others resistant. Our data suggest that resistance is likely mediated in part by type III IFNs. Thus, we provide a potential explanation as to why some individuals may be able to control initial SARS-CoV-2 infection.

The household secondary attack rate for SARS-CoV-2 is estimated to be 16.6%, higher than that of SARS-CoV (7.5%) and MERS (4.7%)[21]. While this demonstrates that household contacts play a significant role in onward transmission of the virus it also highlights that not everyone, despite close contact with an infected individual, will be infected with SARS-CoV-2. Studies on pre-existing immunity to SARS-CoV-2 infections have focused on aspects of the adaptive immune system and have demonstrated reactive T cells in SARS-CoV-2-naive patients being important, possibly due to prior infections with an endemic coronavirus[22]. However, differences in susceptibility to infection due to innate immunity have not been reported previously. Interestingly, a recent pre-print demonstrates a link between inter-individual differences in the expression of anti-SARS-CoV-2 alleles of OAS1 in determine IFN-mediated cellular resistance to infection and subsequent disease[23]. However, in our system, we observed enhanced endogenous secretion of IFN and downstream antiviral ISGs. We propose that resistance to SARS-CoV-2 infection is, in part, due to endogenous secretion and signaling of relatively high

levels type III IFN in the mucosae independent of SARS-CoV-2 infection. This fits with recent work showing high sensitivity of SARS-CoV-2 to prophylactic IFN treatment. SARS-CoV-2 sensitivity to type I and III IFN treatment was previously reported. However, contrary to our findings, these authors did not observe an interferon response to SARS-CoV-2 infection of primary human airway epithelial cells[17]. A study by Dee et al. demonstrated that rhinovirus infection induced an IFN response that blocked subsequent SARS-CoV-2 infection. They proposed that given the prevalence of rhinovirus infections within the population, it could impact the number of COVID-19 cases[24]. In our model, the underlying cause of such IFN secretion remains to be elucidated. Although this phenomenon has only been observed in nasal cells from one donor it provides an exciting precedent to explain resistance to SARS-CoV-2 infection. A large-scale study to determine the frequency of endogenously-activated IFN responses may help to further elucidate and explain differential susceptibility to COVID-19 disease in humans.

WD-PNECs that were resistant to SARS-CoV-2 infection were derived from a donor with no known history of SARS-CoV-2 infection, was unvaccinated against COVID-19 at the time of both nasal brush samplings, and was otherwise in good health. We cannot discount the possibility that the donor had a prior bacterial or viral infection that, while still allowing the epithelial cells to grow and differentiate, resulted in IFNλ production in uninfected WD-PNEC cultures. Furthermore, cultures were grown and differentiated in the presence of antibiotics. Similarly, epigenetic changes are known to occur following viral infection. Of particular note is influenza-induced epigenetic methylation of H3K79, which may play an important role in interferon signaling[25]. That the WD-PNECs cultured from the second nasal brushing 4 months after the initial sample were also resistant to SARS-CoV-2 infection, suggests that this high endogenous level of IFNλ was not a transient response, consistent with a genetic or epigenetic mechanism. Indeed, SNP analysis highlighted differences in IFN pathway genes in the donor that was resistant to SARS-CoV-2 infection compared to those who were permissive. The presence of SNPs in Toll-like receptors (TLRs) is known to affect susceptibility to disease[26]. Here we identified several SNPs unique to donor 122 in TLR1, 2 and 3. Of particular note is a common variant (minor allele frequency of ~0.3 globally) in TLR3 (rs3775291; C>T) which may confer resistance to HIV infection[27]. The mechanism of HIV resistance is still

248 unknown. However, heterozygous individuals have higher cytokine mRNA levels
249 compared to C homozygotes which could restrict viral infection[28]. This phenomenon
250 appears to be virus specific as the same mutation actually confers susceptibility to
251 enteroviral infection[29].

252 Treatment of human CoV infection with recombinant interferon is not a new concept. Type
253 I IFNs were tested against both SARS-CoV and MERS-CoV with promising pre-clinical
254 results but efficacy was less convincing in clinical trials[30,31]. Early clinical trials assessing
255 the efficacy of type I IFN treatment for COVID-19, alone or in combination with other
256 pharmaceuticals, have initially proved promising but further data are needed to draw
257 definitive conclusions. Similarities between type I and III IFN-induced signaling and
258 induction of antiviral and inflammatory responses are well known. However, type III IFN
259 effects are greatest in mucosal tissues, coincident with the tissue location of its receptor
260 on epithelial cells. Induction of type III IFNs results in prolonged expression of ISGs[32,33].
261 Type III IFNs have been trialed for treatment of hepatitis C virus (HCV), and hepatitis delta
262 virus (HDV) and, more recently, SARS-CoV-2, with positive results[34–36]. Type III IFNs,
263 with tissue-restricted receptor expression, are potentially a much more attractive option
264 for treatment of viral infection than the more inflammatory type I IFNs with ubiquitous
265 receptor expression. Our data supports further investigation into IFNλ, directed towards
266 the luminal surface of the airways, to reduce the incidence of severe COVID-19. Here we
267 have identified donor-specific resistance to SARS-CoV-2 infection in WD-PNECs
268 concurrent with high endogenous IFNλ, likely due to genetic differences. These findings
269 point to a previously overlooked mechanism of resistance that could be operating on a
270 global population level.

271

Methods

Virus cultivation and titration

The SARS-CoV-2 clinical isolate BT20.1 was isolated from a patient admitted to Royal Victoria Hospital, Belfast in June 2020. Characterisation of this strain has previously been described[37]. The virus was passaged 4 times on Vero cells, including isolation. The titres of the virus stocks and experimental samples were determined by plaque assay. In brief, Vero cells were seeded at $5x10^4$ cells/well in a 24-well cell culture plate. Twenty-four hours later a 1:10 serial dilution of the virus stock or sample was prepared and inoculated onto the Vero cells. Following 1 h incubation at 37^{o}C a semi-solid agarose overlay was added. Vero cells were further incubated for 3 days then fixed with paraformaldehyde (final concentration 4% v/v) and stained with crystal violet (5% w/v) for plaque visualisation. The origin and characterization of the clinical isolate RSV BT2a were previously described[38]. RSV titres in biological samples were determined using HEp-2 cells, as previously described[39].

Well-differentiated primary nasal epithelial cell (WD-PNEC) culture, infection and treatment

Nasal epithelial cells were obtained from consented healthy adults with no known history of lung disease or previous SARS-CoV-2 infection. Culture and differentiation protocols were previously described[40,41]. In brief, cells were passaged three times in Promocell Airway Epithelial Cell Growth Medium (Promocell) then seeded onto collagen-coated Transwell supports (Corning) at $3x10^4$ cells per Transwell. After 4–6 days of submersion air-liquid interface (ALI) was initiated by removing the apical medium. Cells were differentiated using Stemcell PneumaCult ALI medium (Stemcell Technologies) supplemented with hydrocortisone and heparin. Basolateral medium was replaced every 2 days. Complete differentiation took a minimum of 21 days. WD-PNEC cultures were only used when hallmarks of excellent differentiation were evident, including extensive apical coverage with beating cilia and obvious mucus production. WD-PNECs were infected with SARS-CoV-2 (MOI=0.1) by the addition of inoculum on the apical surface

and incubation for 1 h at 37ºC. Cultures were treated basolaterally with 0, 1 or 100 ng/mL human IFNλ3 (R&D systems, Biotechne) for 24 h. Ruxolitinib (Selleck Chemicals) (1 μM) was added to the basolateral medium 48 h before infection and was replaced at 1 and 48 hpi. Apical washes were harvested by adding 200 μL DMEM (low glucose; Gibco), incubation for 5 mins and gentle aspiration without damaging the cultures.

Immunofluorescence

Cultures were fixed with 4% paraformaldehyde (w/v) for a minimum of 1 hour. Cells were permeabilised with 0.2% Triton X-100 (v/v) then blocked using 0.4% bovine serum albumin (BSA) (w/v). Antibodies used are specified in figure legend. Cells were counterstained with DAPI-mounting medium (Vectashield). Images were obtained on a Nikon Eclipse TE-2000U or a Leica SP5 confocal microscope.

Sequencing and Transcriptomic analysis

WD-PNECs derived from 4 donors were infected with SARS-CoV-2 (MOI=0.1) or mock infected. RNA was extracted at 48 and 96 h for each condition, in duplicate. Cultures were incubated with 400 μl of Lysis/Binding buffer (High Pure Isolation Kit; Roche) for 5 min at RT. Total Lysed samples were vortexed for 15 sec and transferred to a High Pure filter tube. RNA was extracted as per the manufacturer's instructions. RNA sequencing was performed via Kapa RNA HyperPrep with RiboErase (Roche). Raw sequence reads were quality checked with FastQC and pre-processed for the sequence cleaning and adapter removal using cutadapt 2.1 and Trim Galore! To remove adapter contamination. (https://www.bioinformatics.babraham.ac.uk/projects/trim_galore/). These pre-processed fastq files were then aligned to the human genome GRCh38v33 using STAR aligner version 2.7.3a[42] using default parameters and subsequently genes were quantified using htseq version 0.11.3[43].

Quantified genes (raw counts) were processed using edgeR[44] for normalisation purposes and transformed into logCPMs (log counts per million). These logCPM values were subsequently used to generate a heatmap using pheatmap package for comparison and visualisation purposes using a selection of interferon related genes extracted from a

328 selection of pathways annotated in WikiPathways and Reactome Pathway Database
329 (WP2113; R-HSA-913531; WP1904; R-HSA-168928; WP4880; WP1835; R-HSA-
330 909733; WP75), ACE2 and TMPRSS2. SNP calling was carried out using ExactSNP
331 program from the subread package using default parameters[45]. To increase the
332 sequencing depth, we merged together all samples from each donor and used the
333 merged file as input for the SNP calling phase. In addition to SNP calling we also
334 annotated the variants identified using SnpEff software and the GRCh38.99 database[46].

335 **ELISA analysis**

336 Concentrations of IFN-λ1 in basolateral medium samples from WD-PNECs were
337 measured using a human IFN-λ1/IL-29 ELISA (Invitrogen) according to the
338 manufacturer's instructions.

339

340

341 **Acknowledgements:**

342 The authors would like to thank the following individuals and groups for their contribution
343 and assistance: QUB FMHLS Genomics Core Technology Unit; QUB staff Grace Roberts,
344 Judit Barabas, Mervyn McCaigue, Cathy Fenning, Nuala McCann and David Norwood for
345 their guidance and assistance with biological safety and maintenance of the BSL3
346 laboratory.

347

348 **Funding:**

349 This study was supported by funding from UKRI/NIHR (MC_PC_19057) to UP and KM;
350 PHA HSCNI R&D Division (COM/5613/20) to UP, KM, LB, CB, and GLC; and generous
351 donations from the public and QUB alumni to the Queen's University Belfast Foundation.
352

References

1. Zhou, P. *et al.* A pneumonia outbreak associated with a new coronavirus of probable bat origin. *Nature* **579**, 270–273 (2020).

2. Zhu, N. *et al.* A Novel Coronavirus from Patients with Pneumonia in China, 2019. *N. Engl. J. Med.* **382**, 727–733 (2020).

3. Xu, Z., Li, S., Tian, S., Li, H. & Kong, L. quan. Full spectrum of COVID-19 severity still being depicted. *The Lancet* **395**, 947–948 (2020).

4. Hamming, I. *et al.* Tissue distribution of ACE2 protein, the functional receptor for SARS coronavirus. A first step in understanding SARS pathogenesis. *J. Pathol.* **203**, 631–637 (2004).

5. Shang, J. *et al.* Cell entry mechanisms of SARS-CoV-2. *Proc. Natl. Acad. Sci. U. S. A.* **117**, 11727–11734 (2020).

6. Del Valle, D. M. *et al.* An inflammatory cytokine signature predicts COVID-19 severity and survival. *Nat. Med.* **26**, 1636–1643 (2020).

7. Leisman, D. E. *et al.* Cytokine elevation in severe and critical COVID-19: a rapid systematic review, meta-analysis, and comparison with other inflammatory syndromes. *The Lancet Respiratory Medicine* **8**, 1233–1244 (2020).

8. Shaw, A. E. *et al.* Fundamental properties of the mammalian innate immune system revealed by multispecies comparison of type I interferon responses. *PLoS Biol.* **15**, e2004086 (2017).

9. Blanco-Melo, D. *et al.* Imbalanced Host Response to SARS-CoV-2 Drives Development of COVID-19. *Cell* **181**, 1036–1045.e9 (2020).

10. Lucas, C. *et al.* Longitudinal analyses reveal immunological misfiring in severe COVID-19. *Nature* **584**, 463–469 (2020).

11. Galani, I. E. *et al.* Untuned antiviral immunity in COVID-19 revealed by temporal type I/III interferon patterns and flu comparison. *Nat. Immunol.* **22**, 32–40 (2021).

12. Sommereyns, C., Paul, S., Staeheli, P. & Michiels, T. IFN-lambda (IFN-lambda) is expressed in a tissue-dependent fashion and primarily acts on epithelial cells in vivo. *PLoS Pathog.* **4**, e1000017 (2008).

13. Jilg, N. *et al.* Kinetic differences in the induction of interferon stimulated genes by interferon-α and interleukin 28B are altered by infection with hepatitis C virus. *Hepatology* **59**, 1250–1261 (2014).

14. Zhou, S. *et al.* A Neanderthal OAS1 isoform protects individuals of European ancestry against COVID-19 susceptibility and severity. *Nat. Med.* **27**, 659–667 (2021).

15. Pfaender, S. *et al.* LY6E impairs coronavirus fusion and confers immune control of viral disease. *Nat. Microbiol.* **5**, 1330–1339 (2020).

16. Winstone, H. *et al.* The Polybasic Cleavage Site in SARS-CoV-2 Spike Modulates Viral Sensitivity to Type I Interferon and IFITM2. *J. Virol.* **95**, (2021).

17. Vanderheiden, A. *et al.* Type I and Type III Interferons Restrict SARS-CoV-2 Infection of Human Airway Epithelial Cultures. *J. Virol.* **94**, (2020).

18. Villenave, R. *et al.* In vitro modeling of respiratory syncytial virus infection of pediatric bronchial epithelium, the primary target of infection in vivo. *Proc. Natl. Acad. Sci. U. S. A.* **109**, 5040–5 (2012).

19. Felgenhauer, U. *et al.* Inhibition of SARS–CoV-2 by type I and type III interferons. *J. Biol. Chem.* **295**, 13958–13964 (2020).

20. Sungnak, W. *et al.* SARS-CoV-2 entry factors are highly expressed in nasal epithelial cells together with innate immune genes. *Nat. Med. 2020 265* **26**, 681–687 (2020).

21. Madewell, Z. J., Yang, Y., Longini, I. M., Halloran, M. E. & Dean, N. E. Household Transmission of SARS-CoV-2: A Systematic Review and Meta-analysis. *JAMA Netw. open* **3**, e2031756 (2020).

22. Grifoni, A. *et al.* Targets of T Cell Responses to SARS-CoV-2 Coronavirus in Humans with COVID-19 Disease and Unexposed Individuals. *Cell* **181**, 1489–1501.e15 (2020).

23. Wickenhagen, A. *et al.* Wickenhagen et al., A Prenylated dsRNA Sensor Protects Against Severe COVID-19 and is Absent in Horseshoe Bats 1 A Prenylated dsRNA Sensor Protects Against Severe COVID-19 and is Absent in Horseshoe Bats. *medRxiv* 2021.05.05.21256681 (2021). doi:10.1101/2021.05.05.21256681

24. Dee, K. *et al.* Human rhinovirus infection blocks SARS-CoV-2 replication within the respiratory epithelium: implications for COVID-19 epidemiology. *J. Infect. Dis.* (2021). doi:10.1093/infdis/jiab147

25. Marcos-Villar, L. *et al.* Epigenetic control of influenza virus: Role of H3K79 methylation in interferon-induced antiviral response. *Sci. Rep.* **8**, 1230 (2018).

26. Skevaki, C., Pararas, M., Kostelidou, K., Tsakris, A. & Routsias, J. G. Single nucleotide polymorphisms of Toll-like receptors and susceptibility to infectious diseases. *Clin. Exp. Immunol.* **180**, 165 (2015).

27. Huik, K. *et al.* Association between TLR3 rs3775291 and resistance to HIV among highly exposed Caucasian intravenous drug users. *Infect. Genet. Evol.* **20**, 78 (2013).

28. M, S. *et al.* A common polymorphism in TLR3 confers natural resistance to HIV-1 infection. *J. Immunol.* **188**, 818–823 (2012).

29. C, G. *et al.* A role for Toll-like receptor 3 variants in host susceptibility to enteroviral myocarditis and dilated cardiomyopathy. *J. Biol. Chem.* **285**, 23208–23223 (2010).

30. Stockman, L. J., Bellamy, R. & Garner, P. SARS: Systematic review of treatment effects. *PLoS Medicine* **3**, 1525–1531 (2006).

31. Omrani, A. S. *et al.* Ribavirin and interferon alfa-2a for severe Middle East respiratory syndrome coronavirus infection: A retrospective cohort study. *Lancet Infect. Dis.* **14**, 1090–1095 (2014).

32. Lazear, H. M., Schoggins, J. W. & Diamond, M. S. Shared and Distinct Functions of Type I and Type III Interferons. *Immunity* **50**, 907–923 (2019).

33. Pervolaraki, K. *et al.* Differential induction of interferon stimulated genes between type I and type III interferons is independent of interferon receptor abundance. *PLoS Pathog.* **14**, e1007420 (2018).

34. Donnelly, R. P., Dickensheets, H. & O'Brien, T. R. Interferon-lambda and therapy for chronic hepatitis C virus infection. *Trends Immunol.* **32**, 443–50 (2011).

35. Giersch, K. *et al.* Both interferon alpha and lambda can reduce all intrahepatic HDV infection markers in HBV/HDV infected humanized mice. *Sci. Reports 2017 71* **7**, 1–11 (2017).

36. Feld, J. J. *et al.* Peginterferon lambda for the treatment of outpatients with COVID-19: a phase 2, placebo-controlled randomised trial. *Lancet Respir. Med.* **9**, 498–510 (2021).

37. Bamford, C. G. G. *et al.* Collaboration Between Host and Viral Factors Shape SARS-CoV-2 Evolution. *bioRxiv* 2021.07.16.452629 (2021). doi:10.1101/2021.07.16.452629

38. Villenave, R. *et al.* Differential cytopathogenesis of respiratory syncytial virus prototypic and clinical isolates in primary pediatric bronchial epithelial cells. *Virol. J.* **8**, 43 (2011).

39. Power, U. F. *et al.* Induction of Protective Immunity in Rodents by Vaccination with a Prokaryotically Expressed Recombinant Fusion Protein Containing a

Respiratory Syncytial Virus G Protein Fragment. *Virology* **230**, 155–166 (1997).

40. Broadbent, L. *et al.* In Vitro Modeling of RSV Infection and Cytopathogenesis in Well-Differentiated Human Primary Airway Epithelial Cells (WD-PAECs). in *Methods in molecular biology (Clifton, N.J.)* **1442**, 119–39 (2016).

41. Broadbent, L. *et al.* Comparative primary paediatric nasal epithelial cell culture differentiation and RSV-induced cytopathogenesis following culture in two commercial media. *PLoS One* **15**, (2020).

42. Dobin, A. *et al.* STAR: Ultrafast universal RNA-seq aligner. *Bioinformatics* **29**, 15–21 (2013).

43. Anders, S., Pyl, P. T. & Huber, W. HTSeq-A Python framework to work with high-throughput sequencing data. *Bioinformatics* **31**, 166–169 (2015).

44. Robinson, M. D., McCarthy, D. J. & Smyth, G. K. edgeR: A Bioconductor package for differential expression analysis of digital gene expression data. *Bioinformatics* **26**, 139–140 (2009).

45. Y, L., GK, S. & W, S. The R package Rsubread is easier, faster, cheaper and better for alignment and quantification of RNA sequencing reads. *Nucleic Acids Res.* **47**, (2019).

46. Cingolani, P. *et al.* A program for annotating and predicting the effects of single nucleotide polymorphisms, SnpEff: SNPs in the genome of Drosophila melanogaster strain w1118; iso-2; iso-3. *Fly (Austin).* **6**, 80 (2012).

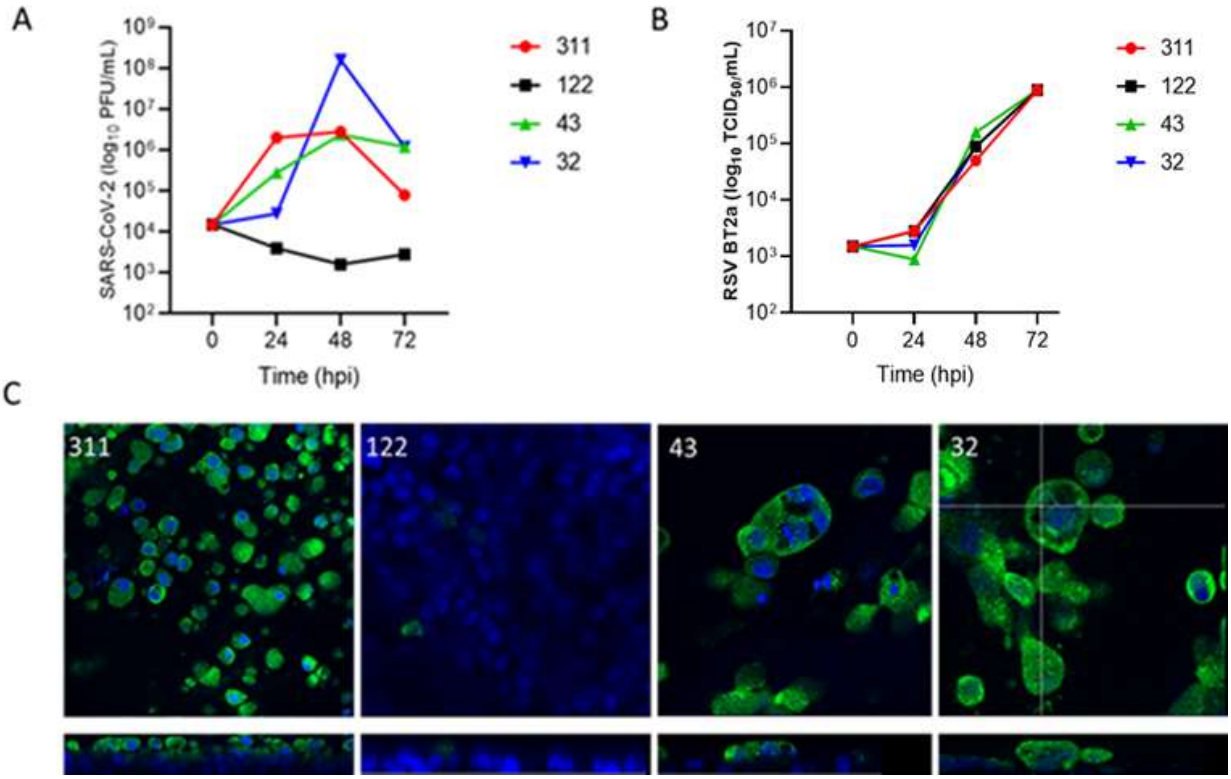

Figure 1: WD-PNECs from different donors are differentially susceptible to SARS-CoV-2, but not RSV.

WD-PNECs from 4 adult donors were infected with a clinical isolate of SARS-CoV-2 (MOI=0.1). Apical washes were harvested every 24 h and titrated by plaque assay on Vero cells (A). Cultures were fixed at 96 hpi and SARS-CoV-2 N protein (green) was detected by immunofluorescence. Nuclei counterstained with DAPI (blue). Images and orthogonal sections were obtained on a Leica SP5 confocal microscope at x63 magnification (B). In parallel, cultures from the same donors were infected with RSV (MOI=0.1). Apical washes were harvested every 24 h and titrated on HEp-2 cells (C).

A

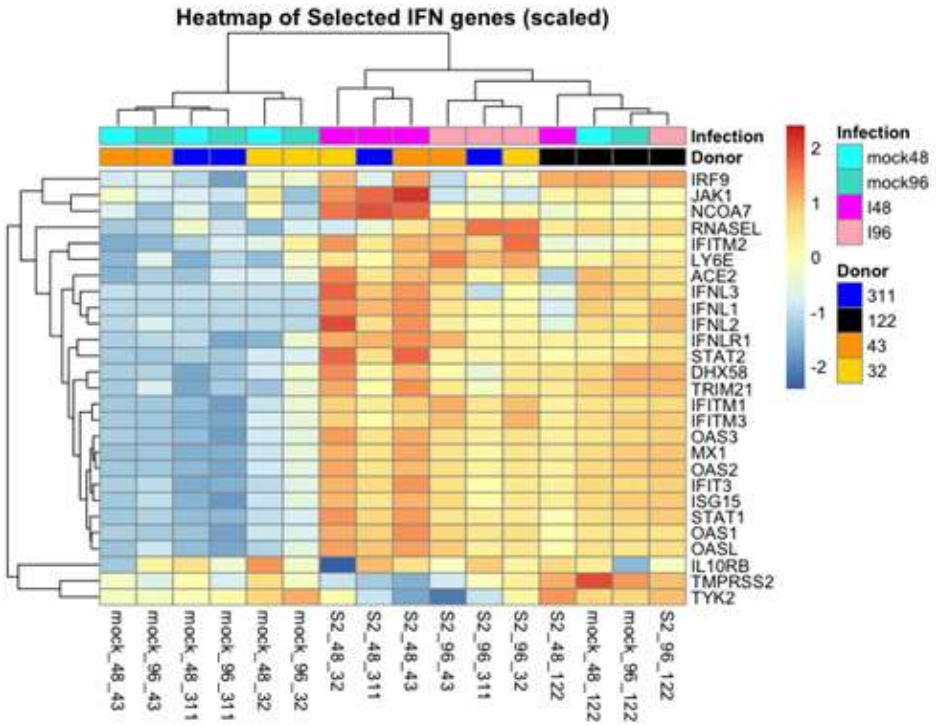

B

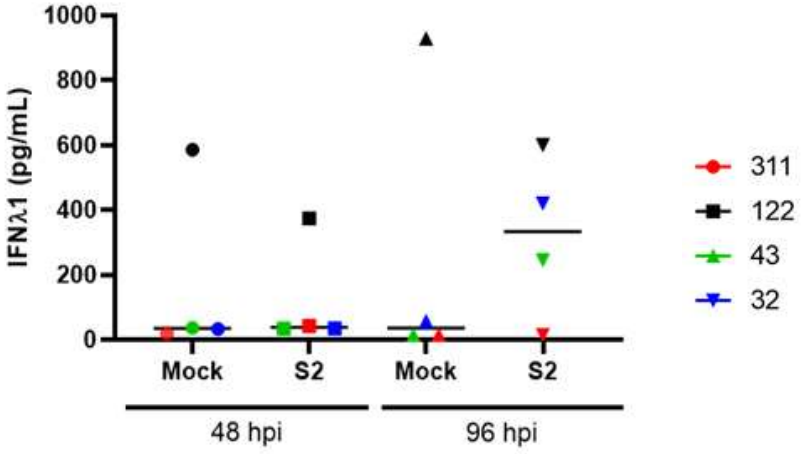

Figure 2. Transcriptomic profiles and protein quantification demonstrated a preactivated IFN response in a donor resistant to infection.

WD-PNECs from 4 adult donors were infected with a clinical isolate of SARS-CoV-2 (MOI=0.1) or mock infected. At 48 and 96 hpi RNA was extracted from the cultures and global transcriptomic analysis was performed. Selected genes, pertaining to innate immune responses to viral infection are illustrated by heatmap, gene upregulation (Red) and down regulation (blue) (A). Preactivated immune response was validated by quantifying IFNλ1 concentration in basolateral medium from mock and SARS-CoV-2 infected WD-PNECs from 4 donors was quantified by ELISA (B).

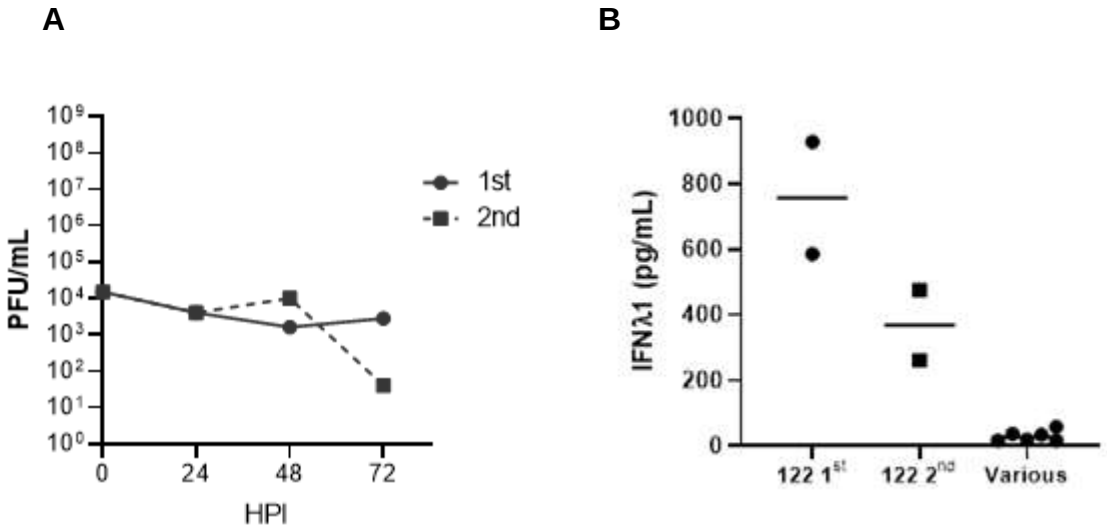

Figure 3. Resistance to SARS-CoV-2 infection and preactivated interferon pathway was not transient

Independent nasal brushes were obtained from donor 122 four months apart, designated 1st brush and 2nd brush (1st brush results from experiment 1A). Cells were cultured for a minimum of 21 days in ALI until fully differentiated then infected with SARS-CoV-2 (MOI=0.1). Apical washes were harvested every 24 hpi up to 72 hpi and titrated by plaque assay. (A). IFNλ concentration in basaolateral medium from uninfected WD-PNECs from the 1st and 2nd nasal brushes from donor 122 were determined by ELISA. This is compared to other uninfected WD-PNEC cultures derived from 6 donors (B).

553

554 **A** **B**

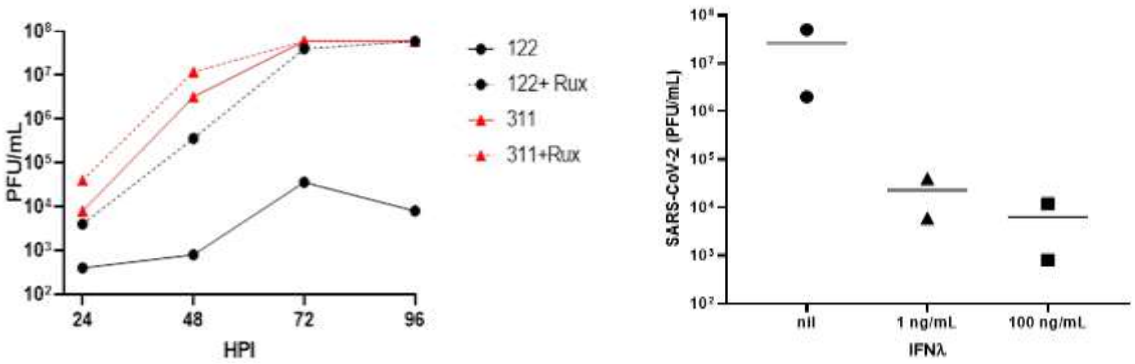

555

556

557 **Figure 4. SARS-CoV-2 growth kinetics are dependent on IFN signalling**. WD-PNECs
558 derived from donor 122 and a permissive donor were treated basolaterally with 1 μM
559 ruxolitinib for 48 h, or left untreated, prior to infection with SARS-CoV-2 (MOI=0.1).
560 Ruxolitinib was replaced at 1 and 48 hpi. Apical washes were harvested every 24 h post
561 infection until 96 hpi. SARS-CoV-2 viral growth kinetics were determined by plaque assay
562 on Vero cells (A). WD-PNECs derived from a SARS-CoV-2 permissive donor were treated
563 basolaterally in duplicate with 0, 1 ng or 100 ng/mL IFNλ for 24 h prior to infection with
564 SARS-CoV-2 (MOI=0.1). Apical washes were harvested at 48 hpi and titrated by plaque
565 assay on Vero cells.

566

567

568

569

570 A

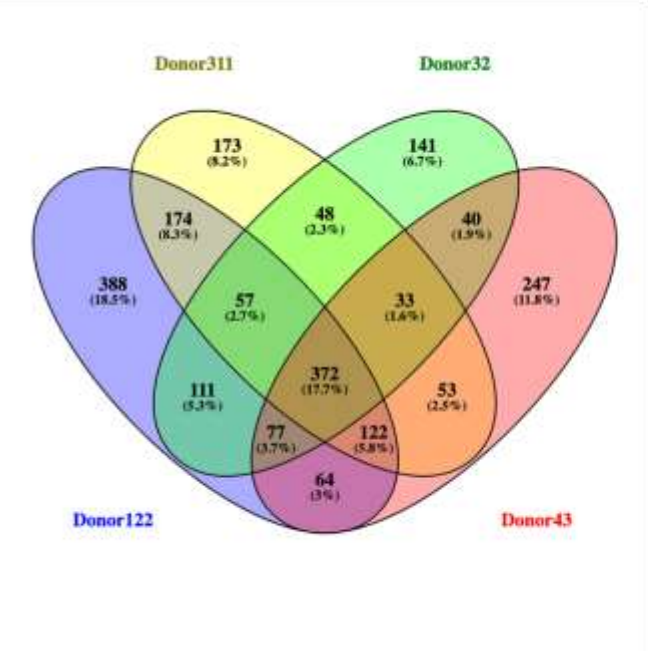

B

SNP	Gene	Donor
rs3738032	ADAR	122
rs1127313	ADAR	311 43 32
rs1127326	ADAR	311 43 32
rs1990760	IFIH1/MDA-5	311 43 32
rs2089960995	MAVS	122
rs4833095	TLR1	122
rs1816702	TLR2	122
rs3804099	TLR2	122
rs3775296	TLR3	122
rs3775291	TLR3	122

571
572 **Figure 5. SNP analysis from transcriptomics data**. SNPs unique to each donor and
573 common displayed as a Venn diagram (A). SNPs unique to donor 122 or not present in
574 donor 122 were filtered by quality (>10), with an existing entry in dbSNP (NIH) and
575 previously published (B).
576
577
578
579
580
581
582
583
584
585
586
587
588
589
590
591
592